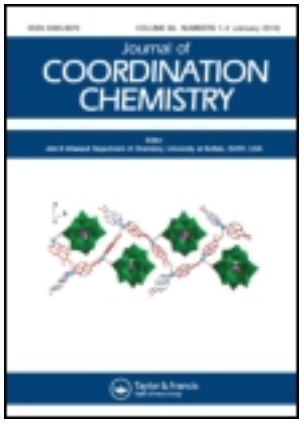

Journal of Coordination Chemistry
Publication details, including instructions for authors and subscription information:
http://www.tandfonline.com/loi/gcoo20

Synthesis and structural characterization of ruthenium complexes with 1-aryl-imidazole-2-thione

Yi Qin [a], Qing Ma [a b], Ai-Quan Jia [a], Qun Chen [a] & Qian-Feng Zhang [a b]

[a] Department of Applied Chemistry, School of Petrochemical Engineering, Changzhou University, Changzhou, P.R. China

[b] Institute of Molecular Engineering and Applied Chemistry, Anhui University of Technology, Ma'anshan, P.R. China

Accepted author version posted online: 06 Mar 2013.Published online: 15 Apr 2013.

To cite this article: Yi Qin, Qing Ma, Ai-Quan Jia, Qun Chen & Qian-Feng Zhang (2013) Synthesis and structural characterization of ruthenium complexes with 1-aryl-imidazole-2-thione, Journal of Coordination Chemistry, 66:8, 1405-1415, DOI: 10.1080/00958972.2013.782607

To link to this article: http://dx.doi.org/10.1080/00958972.2013.782607

Journal of Coordination Chemistry, 2013
Vol. 66, No. 8, 1405–1415, http://dx.doi.org/10.1080/00958972.2013.782607

Synthesis and structural characterization of ruthenium complexes with 1-aryl-imidazole-2-thione

YI QIN†, QING MA†‡, AI-QUAN JIA†, QUN CHEN† and QIAN-FENG ZHANG*†‡

†Department of Applied Chemistry, School of Petrochemical Engineering, Changzhou University, Changzhou, P.R. China
‡Institute of Molecular Engineering and Applied Chemistry, Anhui University of Technology, Ma'anshan, P.R. China

(*Received 10 September 2012; in final form 17 January 2013*)

Treatment of $[RuCl_2(PPh_3)_3]$ with 2 equiv. $Himt^{MPh}$ ($Himt^{MPh}$ = 1-(4-methyl-phenyl)-imidazole-2-thione) in the presence of MeONa afforded *cis*-$[Ru(\kappa^2\text{-}S,N\text{-}imt^{MPh})_2(PPh_3)_2]$ (**1**), while interaction of $[RuCl_2(PPh_3)_3]$ and 2 equiv. $Himt^{MPh}$ in tetrahydrofuran (THF) without base gave $[RuCl_2(\kappa^1\text{-}S\text{-}Himt^{MPh})_2(PPh_3)_2]$ (**2**). Treatment of $[RuHCl(CO)(PPh_3)_3]$ with 1 equiv. $Himt^{MPh}$ in THF gave $[RuHCl(\kappa^1\text{-}S\text{-}Himt^{MPh})(CO)(PPh_3)_2]$ (**3**), whereas reaction of $[RuHCl(CO)(PPh_3)_3]$ with 1 equiv. of the deprotonated $[imt^{MPh}]^-$ or $[imt^{NPh}]^-$ (imt^{NPh} = 1-(4-nitro-phenyl)-2-mercaptoimidazolyl) gave $[RuH(\kappa^2\text{-}S,N\text{-}imt^{RPh})(CO)(PPh_3)_2]$ (R = M **4a**, R = N **4b**). The ruthenium hydride complexes **4a** and **4b** easily convert to their corresponding ruthenium chloride complexes $[RuCl(\kappa^2\text{-}S,N\text{-}imt^{MPh})(CO)(PPh_3)_2]$ (**5a**) and $[RuCl(\kappa^2\text{-}S,N\text{-}imt^{NPh})(CO)(PPh_3)_2]$ (**5b**), respectively, in refluxing $CHCl_3$ by chloride substitution of the RuH. Photolysis of **5a** in $CHCl_3$ at room temperature afforded an oxidized product $[RuCl_2(\kappa^2\text{-}S,N\text{-}imt^{MPh})(PPh_3)_2]$ (**6**). Reaction of **6** with excess $[imt^{MPh}]^-$ afforded **1**. The molecular structures of **1**·EtOH, **3**·C_6H_{14}, **4b**·0.25CH_3COCH_3, and **6**·2CH_2Cl_2 have been determined by single-crystal X-ray crystallography.

Keywords: Ruthenium complex; Imidazole-2-thione ligand; Synthesis; Crystal structure

1. Introduction

Coordination chemistry of heterocyclic thiones containing –N(H)=C(=S)– ↔ –N=C(–SH)– is of considerable interest because such compounds show similar cysteine sulfur coordination in metalloenzymes [1] and the structural properties of the *S*,*N*-coordination active sites [2–4]. Accordingly, substituted imidazole-2-thiones are important ligands due to coordination with a variety of donor atoms [5] and their numerous biochemical properties [6]; they can further form stable complexes with a wide range of main group and transition metal ions [7–12]. Thus, exploration of the coordination properties of thione donors toward metal ions is extensive [2–12]; however, relatively few ruthenium-thione complexes have been synthesized. Examples of structurally characterized ruthenium-thione complexes include $[Ru(R)(\kappa^2\text{-}S,N\text{-}mt)(CO)(PPh_3)_2]$ (R=H, $CH{=}CH_2$, CH=CHPh, $CH{=}CH{-}C_6H_4CH_{3-4}$, $CH{=}CH^tBu$, $CH{=}CHCPh_2OH$, $C(C{\equiv}CPh){=}CHPh$, C_6H_5, $C{\equiv}CPh$, $SiMe_2OEt$) [13],

*Corresponding author. Email: zhangqf@ahut.edu.cn

[Ru(κ^2-*S,N*-mt)$_2$(PPh$_3$)$_2$] [10], and [RuH(κ^2-*S,N*-mt)(PPh$_3$)$_3$] [11] (mt = *N*-methyl-2-mercaptoimidazolyl).

Transition metal hydride complexes are of importance in many stoichiometric and catalytic reactions. For example, they are involved in catalytic hydrogenation, hydrosilylations, hydroformylation, polymerization, and hydrogen transferring reactions [14]. In recent years, there has been interest in ruthenium hydride complexes relative to deprotonation [15], insertion [16], and protonation [17]. Low-valent ruthenium hydrides can be used as alternatives to conventional Lewis acids and bases [18]; in particular, [RuHCl(CO)(PPh$_3$)$_3$] may catalyze addition of aldehydes to dienes and -alkylation of ketones with primary alcohols [19, 20], and [RuH$_2$(PPh$_3$)$_4$] may catalyze hydration of nitriles to give the corresponding amides [21]. In the course of our research on ruthenium hydride complexes in electron-rich sulfur coordination environments [22, 23], we became interested in reactivity and structural characterization of ruthenium hydride complexes with substituted imidazole-2-thione ligands [24, 25]. In this paper, the coordination properties of 1-aryl-imidazole-2-thiones to ruthenium with triphenyl-phosphines as co-ligands along with photo-oxidation of the ruthenium carbonyl complex and ligand-reduction in ruthenium chloride complexes are described.

2. Experimental

2.1. *General*

All syntheses were carried out under dry nitrogen by standard Schlenk techniques. 4-Methyl-phenyl-amine, 4-nitro-phenyl-amine, and amino acetal were purchased from Alfa Aesar Ltd. and used without purification. 1-(4-Methyl-phenyl)-imidazole-2-thione (Himt^{MPh}) [26], 1-(4-nitro-phenyl)-imidazole-2-thione (Himt^{NPh}) [26], [RuCl$_2$(PPh$_3$)$_3$] [27], and [RuHCl(CO)(PPh$_3$)$_3$] [28] were prepared according to literature methods. NMR spectra were recorded on a Bruker ALX 400 Plus spectrometer operating at 400 and 162 MHz for ^{1}H and ^{31}P, respectively. Chemical shifts (δ, ppm) were reported with reference to SiMe$_4$ (^{1}H) and H$_3$PO$_4$ (^{31}P). Infrared spectra (KBr) were recorded on a PerkinElmer 16 PC FT-IR spectrophotometer using pressed KBr pellets, and positive FAB mass spectra were recorded on a Finnigan TSQ 7000 spectrometer. The magnetic moment for the solid sample was measured by a Sherwood magnetic susceptibility balance at room temperature. The photolysis source was the output from a 100 W high-pressure mercury lamp passed through an IR filter and collimated with lenses. An appropriate interference filter was used to select the desired λ_{irr}. A shutter shielded the sample from the arc lamp. Elemental analyses were carried out using a PerkinElmer 2400 CHN analyzer.

2.2. *Synthesis of cis-[Ru(κ2-S,N-imtMPh)2(PPh3)2]·EtOH (1·EtOH)*

To a slurry of Himt^{MPh} (38 mg, 0.20 mM) and MeONa (10.8 mg, 0.20 mM) in tetrahydrofuran (THF) (5 mL) was added a solution of [RuCl$_2$(PPh$_3$)$_3$] (96 mg, 0.10 mM) in THF (10 mL). The mixture was stirred for 8 h at room temperature. The solvent was removed in vacuo, and the residue was washed with hexane. The residue was extracted with dichloromethane and filtered; the solvent was removed in vacuo and further recrystallized from CH$_2$Cl$_2$/EtOH/Et$_2$O at room temperature. Block orange crystals of **1**·EtOH suitable for X-ray diffraction were obtained in a week. Yield: 90 mg, 86%. ^{31}P NMR (*C*DCl$_3$): 29.2,

55.6 ppm. ^{1}H NMR (C*D*Cl$_3$): 1.25 (EtOH), 2.35 (s, Me, 6H), 3.72 (EtOH), 6.31 (s, *imt*-CH, 2H), 6.50 (d, *imt*-CH, J = 1.6 Hz, 2H), 6.96–6.70 (m, 12H), 7.09–7.13 (m, 6H), 7.19 (d, C_6H_4, J = 8.0 Hz, 4H), 7.26–7.30 (m, 16H) ppm. IR (KBr disk, cm^{-1}): 3052 (w), 1634 (m), 1595 (m), 1499 (s), 1432 (s), 1362 (s), 1263 (s), 1098 (s), 1031 (s), 805 (s), 694 (s), 538 (s), 524 (s), 500 (m). MS (FAB): *m/z* 1052 [M$^+$], 790 [M$^+$ – PPh$_3$], 528 [M$^+$ – 2PPh$_3$]. Anal. Calcd for $C_{56}H_{48}N_4P_2S_2Ru\cdot(C_2H_6O)$ (%): C, 66.20; H, 5.36; N, 5.32. Found: C, 66.11; H, 5.34; N, 5.35.

2.3. *Synthesis of [RuCl$_2$(κ^1-S-Himt^{MPh})$_2$(PPh$_3$)$_2$] (2)*

A mixture of [RuCl$_2$(PPh$_3$)$_3$] (96 mg, 0.10 mM) and Himt^{MPh} (38 mg, 0.20 mM) in THF (15 mL) was refluxed with stirring for 1 h, during which there was a color change from dark red to orange red. The solvent was removed in vacuo, and the residue was washed with diethyl ether and hexane. Recrystallization from CH_2Cl_2/hexane afforded yellow microcrystals of **2**. Yield: 86 mg, 80%. ^{31}P NMR (C*D*Cl$_3$): 29.3 (s) ppm. ^{1}H NMR (C*D*Cl$_3$): 2.34 (s, Me, 6H), 5.60 (s, *imt*-CH, 2H), 6.58 (s, *imt*-CH, 2H), 6.86 (d, C_6H_4, 4H, J = 8.0 Hz), 7.10 (d, C_6H_4, 4H, J = 8.0 Hz), 7.28–7.54 (m, PPh$_3$, 30H), 11.64 (br s, NH, 2H) ppm. IR (KBr disk, cm^{-1}): 3150 (w), 3110 (w), 3049 (w), 1629 (m), 1592 (m), 1495 (s), 1435 (s), 1322 (m), 1255 (s), 1094 (s), 1020 (s), 799 (s), 746 (s), 715 (s), 696 (s), 543 (s). MS (FAB): *m/z* 1077 [M$^+$], 1042 [M$^+$ – Cl], 1007 [M$^+$ – 2Cl], 815 [M$^+$ – PPh$_3$], 555 [M$^+$ – 2PPh$_3$], 483 [M$^+$ – 2Cl – 2PPh$_3$]. Anal. Calcd for $C_{56}H_{50}N_4Cl_2P_2S_2Ru$ (%): C, 62.45; H, 4.68; N, 5.20. Found: C, 62.49; H, 4.71; N, 5.26.

2.4. *Synthesis of [RuHCl(κ^1-S-imt^{MPh})(CO)(PPh$_3$)$_2$]·C$_6$H$_{14}$ (3·C$_6$H$_{14}$)*

A mixture of [RuHCl(CO)(PPh$_3$)$_3$] (95 mg, 0.10 mM) and Himt^{MPh} (30 mg, 0.16 mM) in THF (15 mL) was stirred at room temperature for 1 h, during which there was a color change from red to yellowish orange. The solvent was removed in vacuo, and the residue was washed with diethyl ether and hexane. Recrystallization from CH_2Cl_2/hexane afforded yellow block-shaped crystals of **3**·C_6H_{14} in a week. Yield: 40 mg, 45%. ^{31}P NMR (C*D*Cl$_3$): 40.9 (s) ppm. ^{1}H NMR (C*D*Cl$_3$): –14.80 (t, J = 22.0 Hz, 1H), 0.88 (C_6H_{14}), 1.26 (C_6H_{14}), 2.32 (s, Me, 3H), 6.19 (s, *imt*-CH, 1H), 6.36 (s, *imt*-CH, 1H), 6.78 (d, C_6H_4, 2H, J = 8.0 Hz), 7.10 (d, C_6H_4, 2H, J = 8.0 Hz), 7.25–7.77 (m × 2, PPh$_3$, 30H), 12.68 (s, NH, 1H) ppm. IR (KBr disk, cm^{-1}): 3137 (w), 3054 (w), 1926 (vs), 1590 (m), 1565 (m), 1499 (s), 1437 (s), 1321 (m), 1265 (s), 1093 (s), 1026 (s), 802 (s), 745 (s), 699 (s), 540 (s), 524 (s), 503 (s). MS (FAB): *m/z* 881 [M$^+$], 879 [M$^+$ – H – 1], 844 [M$^+$ – H – Cl], 816 [Ru(κ^1-*S*-imt^{MPh})(PPh$_3$)$_2$]$^+$, 554 [Ru(κ^1-*S*-imt^{MPh})(PPh$_3$)]$^+$, 292 [Ru(κ^1-*S*-imt^{MPh})]$^+$. Anal. Calcd for $C_{47}H_{41}N_2OClP_2SRu\cdot(C_6H_{14})$ (%): C, 65.86; H, 5.74; N, 2.90. Found: C, 65.78; H, 5.78; N, 2.86.

2.5. *Synthesis of [RuH(κ^2-S,N-imt^{MPh})(CO)(PPh$_3$)$_2$] (4a)*

To a slurry of Himt^{MPh} (19 mg, 0.10 mM) and MeONa (5.4 mg, 0.10 mM) in THF (5 mL) was added a solution of [RuHCl(CO)(PPh$_3$)$_3$] (95 mg, 0.10 mM) in THF (10 mL). The mixture was stirred for 2 h at room temperature. The solvent was removed in vacuo, and the residue was washed with hexane and further recrystallized from CH_2Cl_2/hexane at room

temperature. Yellow crystalline product of **4a** was obtained in three days. Yield: 42 mg, 50%. ^{31}P NMR (C*D*Cl$_3$): 39.3 (s) ppm. ^{1}H NMR (C*D*Cl$_3$): −14.30 (t, RuH, J = 22.5 Hz, 1H), 2.30 (s, Me, 3H), 6.04 (d, *im*-CH, J = 2.0 Hz, 1H), 6.37 (d, *im*-CH, J = 2.0 Hz, 1H), 6.68 (d, C_6H_4, 2H, J = 8.4 Hz), 7.10 (d, C_6H_4, 2H, J = 8.8 Hz), 7.32–7.58 (m × 2, PC_6H_5, 30H) ppm. IR (KBr disk, cm^{-1}): 1927 (vs), 1593 (m), 1565 (m), 1503 (s), 1436 (s), 1321 (m), 1264 (s), 1098 (s), 1021 (s), 801 (s), 746 (s), 697 (s), 540 (s), 524 (s), 502 (s). MS (FAB): *m/z* 844 [M$^+$], 842 [M$^+$ – H – 1], 808 [M$^+$ – H – Cl], 814 [Ru(κ^2-*S*,*N*-imt^{MPh})(PPh$_3$)$_2$]$^+$, 552 [Ru(κ^2-*S*,*N*-imt^{MPh})(PPh$_3$)]$^+$, 291 [Ru(κ^2-*S*,*N*-imt^{MPh})]$^+$. Anal. Calcd for $C_{47}H_{40}N_2OP_2SRu$ (%): C, 66.89; H, 4.78; N, 3.32. Found: C, 66.79; H, 4.76; N, 3.35.

2.6. *Synthesis of [RuH(κ^2-S,N-Himt^{NPh})(CO)(PPh$_3$)$_2$]·0.25CH$_3$COCH$_3$ (4b·0.25CH$_3$COCH$_3$)*

To a slurry of Himt^{NPh} (22 mg, 0.10 mM) and MeONa (5.4 mg, 0.10 mM) in THF (5 mL) was added a solution of [RuHCl(CO)(PPh$_3$)$_3$] (95 mg, 0.10 mM) in THF (10 mL). The mixture was stirred for 6 h at room temperature. The solvent was removed in vacuo and the residue was washed with hexane and further recrystallized from CH$_3$COCH$_3$/hexane at room temperature. Orange crystals of **4b**·0.25CH$_3$COCH$_3$ were obtained in a week. Yield: 52 mg, 60%. ^{31}P NMR (C*D*Cl$_3$): 39.2 (s) ppm. ^{1}H NMR (C*D*Cl$_3$): −14.28 (t, RuH, J = 22.0 Hz, 1H), 2.10 (CH$_3$COCH$_3$), 6.03 (d, *im*-CH, J = 2.0 Hz, 1H), 6.34 (d, *im*-CH, J = 2.0 Hz, 1H), 6.69 (d, C_6H_4, 2H, J = 8.4 Hz), 7.25–7.58 (m × 2, PC_6H_5, 30H), 8.14 (d, C_6H_4, 2H, J = 8.4 Hz) ppm. IR (KBr disk, cm^{-1}): 1930 (vs), 1595 (m), 1565 (m), 1504 (s), 1435 (s), 1324 (m), 1265 (s), 1098 (s), 1021 (s), 800 (s), 748 (s). MS (FAB): *m/z* 875 [M$^+$], 873 [M$^+$ – H – 1], 839 [M$^+$ – H – Cl], 845 [Ru(κ^2-*S*,*N*-imt^{NPh})(PPh$_3$)$_2$]$^+$, 583 [Ru(κ^2-*S*,*N*-imt^{NPh})(PPh$_3$)]$^+$, 322 [Ru(κ^2-*S*,*N*-imt^{NPh})]$^+$. Anal. Calcd for $C_{46}H_{37}N_3O_3P_2S$-Ru·(0.25C_3H_6O) (%): C, 63.12; H, 4.36; N, 4.72. Found: C, 63.09; H, 4.38; N, 4.75.

2.7. *Synthesis of [RuCl(κ^2-S,N-imt^{MPh})(CO)(PPh$_3$)$_2$] (5a)*

4a (75 mg, 0.1 mM) was refluxed in 5 mL CHCl$_3$ for 1 h. After the mixture was cooled to room temperature, the solvent was removed in vacuo and the residue was washed with hexane, giving the yellow powder. Yield: 64 mg, 82%. ^{31}P NMR (C*D*Cl$_3$): 38.4 (s) ppm. ^{1}H NMR (C*D*Cl$_3$): 2.28 (s, Me, 3H), 5.90 (d, *im*-CH, 1H, J = 2.0 Hz), 6.26 (d, *im*-CH, 1H, J = 1.6 Hz), 6.69 (d, C_6H_4, 2H, J = 8.8 Hz), 7.03 (d, C_6H_4, 2H, J = 8.0 Hz), 7.22–7.28, 7.58–7.63 (m × 2, PC_6H_5, 30H) ppm. ^{13}C NMR (C*D*Cl$_3$): δ 206.2 (t, CO, J_{Cp} = 15.8 Hz), 152.0 (s, NCN), 136.8 (s, *ipso*-C_6H_4), 134.9 (t, *o/m*-PC_6H_5, J_{Cp} = 5.5 Hz), 134.1 (s, *o/m*-C_6H_4), 133.1 (t, *ipso*-PC_6H_5, J_{Cp} = 21.7 Hz), 130.1 (s, *o/m*-C_6H_4), 129.9 (s, *p*-PC_6H_5), 128.1 (t, *o/m*-PC_6H_5, J_{Cp} = 4.8 Hz), 125.6 (s, *p*-C_6H_4), 121.8 (s, NC^{4}H), 114.9 (s, NC^{5}H), 21.4 (s, Me) ppm. IR (KBr disk, cm^{-1}): 1919 ν(CO) cm^{-1}. MS (FAB): *m/z* 777 [M$^+$], 742 [M$^+$ – Cl], 515 [M$^+$ – PPh$_3$], 253 [M$^+$ – 2PPh$_3$], 218 [M$^+$ – Cl – 2PPh$_3$]. Anal. Calcd for $C_{47}H_{39}ClN_2OP_2RuS$: C, 64.27; H, 4.48; N, 3.19. Found: C, 64.19; H, 4.44; N, 3.23.

2.8. *Synthesis of [RuCl(κ^2-S,N-imt^{NPh})(CO)(PPh$_3$)$_2$] (5b)*

The method was similar to that used for **5a**, employing **4b** (78 mg, 0.1 mM) instead of **4a**. Yield: 70 mg, 85%. ^{31}P NMR (C*D*Cl$_3$): 38.2 ppm. ^{1}H NMR (C*D*Cl$_3$): 6.03 [d, *im*-CH, 1H,

$J = 1.6$ Hz], 6.32 [d, *im*-CH, 1H, $J = 1.6$ Hz], 6.71 [d, C_6H_4, 2H, $J = 3.7$ Hz], 7.24–7.29, 7.57–7.62 [m × 2, PC_6H_5, 30H], 8.12 [d, C_6H_4, 2H, $J = 3.6$ Hz] ppm. ^{13}C NMR ($CDCl_3$): δ 205.3 [t, CO, $J_{Cp} = 15.3$ Hz], 152.9 [s, NCN], 145.1 [s, *ipso*-C_6H_4], 141.2 [s, *p*-C_6H_4], 134.4 [t, *o/m*-PC_6H_5, $J_{Cp} = 5.4$ Hz], 132.4 [t, *ipso*-PC_6H_5, $J_{Cp} = 21.9$ Hz], 129.6 [s, *p*-PC_6H_5], 127.6 [t, *o/m*-PC_6H_5, $J_{Cp} = 4.8$ Hz], 126.3 [s, *o/m*-C_6H_4], 124.9 [s, *o/m*-C_6H_4], 120.6 [s, NC^4H], 113.4 [s, NC^5H] ppm. IR (KBr disk, cm^{-1}): 1940 ν(CO) cm^{-1}. MS (FAB): *m/z* 820 [M^+], 785 [M^+ – Cl], 558 [M^+ – PPh_3], 296 [M^+ – $2PPh_3$], 261 [M^+ – Cl – $2PPh_3$]. Anal. Calcd for $C_{46}H_{36}ClN_3O_3P_2RuS$: C, 60.72; H, 3.99; N, 4.62. Found: C, 60.45; H, 4.03; N, 4.67.

2.9. *Synthesis of [RuCl$_2$(κ^2-S,N-imt^{MPh})(PPh$_3$)$_2$]·2CH$_2$Cl$_2$ (6·2CH$_2$Cl$_2$)*

A solution of **5a** (45 mg, 0.058 mM) in $CHCl_3$ (25 mL) was irradiated with UV light under N_2 for 1 h, during which time the color changed from yellow to orange and further to green. The solvent was filtered and pumped off, and the residue was washed with hexane and then further recrystallized from CH_2Cl_2/hexane at room temperature. Air-stable green crystals of **6**·$2CH_2Cl_2$ suitable for X-ray diffraction were obtained in three days. Yield: 34 mg, 75%. Magnetic moment $\mu_{eff} = 1.95$ μ_B at 296 K. IR (KBr disk, cm^{-1}): 1636 (m), 1592 (m), 1495 (s), 1431 (s), 1365 (s), 1262 (s), 1091 (s), 1034 (s), 805 (s), 692 (s), 540 (s), 524 (s), 503 (m). MS (FAB): *m/z* 886 [M^+], 851 [M^+ – Cl], 816 [M^+ – 2Cl]. Anal. Calcd for $C_{46}H_{39}N_2Cl_2P_2SRu·(2CH_2Cl_2)$ (%): C, 54.61; H, 4.11; N, 2.65. Found: C, 54.69; H, 4.12; N, 2.68.

2.10. *Reaction of 6 and Na[imt^{MPh}]*

To a slurry of Himt^{MPh} (38 mg, 0.20 mM) and MeONa (11 mg, 0.20 mM) in THF (5 mL) was added a solution of **6** (78 mg, 0.10 mM) in CH_2Cl_2 (5 mL). The mixture was refluxed with stirring for 2 h, during which there was a color change from green to orange red. The solvent was removed in vacuo, and the residue was washed with diethyl ether and hexane. Recrystallization from CH_2Cl_2/hexane afforded orange crystals that were identified as **1** by using unit cell measurement and elemental analyses. Yield: 84 mg, 80%.

2.11. *X-ray crystallography*

A summary of crystallographic data and experimental details for **1**·EtOH, **3**·C_6H_{14}, **4b**·$0.25CH_3COCH_3$ and **6**·$2CH_2Cl_2$ is summarized in table 1. Intensity data were collected on a Bruker SMART APEX 2000 CCD diffractometer using graphite-monochromated Mo-Kα radiation ($\lambda = 0.71073$ Å) at 293(2) K. The collected frames were processed with SAINT [29]. The data were corrected for absorption using SADABS [30]. Structures were solved by direct methods and refined by full-matrix least-squares on F^2 using the SHELXTL software package [31, 32]. All non-hydrogen atoms were refined anisotropically. The positions of all hydrogens were generated geometrically (C_{sp3}–H = 0.96 and C_{sp2}–H = 0.93 Å), assigned isotropic thermal parameters, and allowed to ride on their respective parent carbon or oxygen before the final cycle of least-squares refinement. The hydrogen on the amino group of **3**·C_6H_{14} was found from subsequent difference Fourier electronic density maps. Solvent molecules such as ethanol in **1**·EtOH and hexane in **3**·C_6H_{14} were

Table 1. Crystallographic data and experimental details for *cis*-[Ru(κ^2-*S*,*N*-imt^{MPh})$_2$(PPh$_3$)$_2$]·EtOH (**1**·EtOH), [RuHCl(κ^1-*S*-imt^{MPh})(CO)(PPh$_3$)$_2$]·C$_6$H$_{14}$ (**3**·C$_6$H$_{14}$), [RuH(κ^2-*S*,*N*-Himt^{NPh})(CO)-(PPh$_3$)$_2$]·0.25CH$_3$COCH$_3$ (**4b**·0.25CH$_3$COCH$_3$), and [RuCl$_2$(κ^2-*S*,*N*-imt^{MPh})(PPh$_3$)$_2$]·2CH$_2$Cl$_2$ (**6**·2CH$_2$Cl$_2$).

Complex	**1**·EtOH	**3**·C$_6$H$_{14}$	**4b**·0.25CH$_3$COCH$_3$	**6**·2CH$_2$Cl$_2$
Empirical formula	$C_{58}H_{48}N_4OP_2S_2Ru$	$C_{50}H_{55}N_2ClOP_2SRu$	$C_{46.75}H_{38.5}N_3O_{3.25}P_2SRu$	$C_{48}H_{43}N_2Cl_6P_2SRu$
Formula weight	1044.13	930.48	889.38	1055.61
Crystal system	Triclinic	Triclinic	Triclinic	Triclinic
a (Å)	11.004(13)	12.567(5)	11.2971(12)	13.461(3)
b (Å)	11.590(13)	13.794(5)	13.1120(13)	14.723(3)
c (Å)	22.71(3)	15.680(5)	15.3496(16)	15.018(5)
α (°)	103.339(15)	66.503(5)	84.238(1)	112.144(3)
β (°)	92.894(14)	72.536(4)	79.400(1)	105.111(3)
γ (°)	107.331(15)	85.293(5)	86.099(1)	105.393(2)
V (Å^3)	2668(5)	2375.6(14)	2220.8(4)	2431.3(10)
Space group	*P*-1	*P*-1	*P*-1	*P*-1
Z	2	2	2	2
D_{calc} (g cm^{-3})	1.300	1.301	1.272	1.442
Temperature (K)	296(2)	273(2)	296(2)	296(2)
F(0 0 0)	1076	968	873	1074
μ (Mo-Kα) (mm^{-1})	0.475	0.535	0.508	0.796
Total refln.	16,229	11,904	13,848	12,519
Independent refln.	11,441	8161	9768	8396
Parameters	607	525	547	524
R_{int}	0.0337	0.0297	0.0158	0.0278
*R*1[a], *wR*2[b] ($I > 2\sigma(I)$)	0.0575, 0.1425	0.0583, 0.1536	0.0376, 0.0995	0.0629, 0.1770
*R*1, *wR*2 (all data)	0.0904, 0.1619	0.0925, 0.1734	0.0479, 0.1075	0.0835, 0.1935
GoF[c]	0.965	0.980	1.011	1.043

[a] $R_1 = \Sigma||F_o| - |F_c||/\Sigma|F_o|$.
[b] $wR_2 = [\Sigma w(|F_o^2| - |F_c^2|)^2/\Sigma w|F_o^2|^2]^{1/2}$.
[c] $GoF = [\Sigma w(|F_o| - |F_c|)^2/(N_{obs} - N_{param})]^{1/2}$.

isotropically refined without hydrogens due to disorder, which probably resulted in the relatively high R values in the final refinement.

3. Results and discussion

Reactions between Himt^{MPh} or Himt^{NPh} and [Ru(PPh$_3$)$_3$Cl$_2$] and [RuHCl(CO)(PPh$_3$)$_3$] along with reactivity of the ruthenium hydride and carbonyl complexes are illustrated in scheme 1. Interaction of [RuCl$_2$(PPh$_3$)$_3$] with 2 equiv. Himt^{MPh} in the presence of MeONa afforded *cis*-[Ru(κ^2-*S*,*N*-imt^{MPh})$_2$(PPh$_3$)$_2$] (**1**). Two chlorides of [RuCl$_2$(PPh$_3$)$_3$] were substituted by two deprotonated [imt^{MPh}]$^-$ resulting in **1** as the only product. The *trans*-isomer could not be isolated either at room temperature or at reflux, suggesting that the *cis*-isomer is the thermodynamic product. **1** is similar to *cis*-[Ru(PPh$_3$)$_2$(κ^2-*S*,*N*-(imt^{Me})$_2$], which was obtained from reaction of [RuCl$_2$(PPh$_3$)$_3$] and Na[HB(tim^{Me})$_3$] [10]. Treatment of [RuCl$_2$(PPh$_3$)$_3$] and 2 equiv. Himt^{MPh} in THF at room temperature gave [RuCl$_2$(κ^1-*S*-Himt^{MPh})$_2$(PPh$_3$)$_2$] (**2**) as the sole isolable product. One PPh$_3$ in the starting ruthenium compound dissociated and two neutral Himt^{MPh} ligands terminally coordinated with ruthenium forming the six-coordinate **2**. Treatment of [RuHCl(CO)(PPh$_3$)$_3$] with 1 equiv. Himt^{MPh} in THF gave [RuHCl(κ^1-*S*-Himt^{MPh})(CO)(PPh$_3$)$_2$] (**3**) as the only product. One PPh$_3$ in the starting ruthenium hydride compound was replaced by one Himt^{MPh}, while interaction of [RuHCl(CO)(PPh$_3$)$_3$] with 1 equiv. of deprotonated [imt^{MPh}] or [imt^{NPh}]

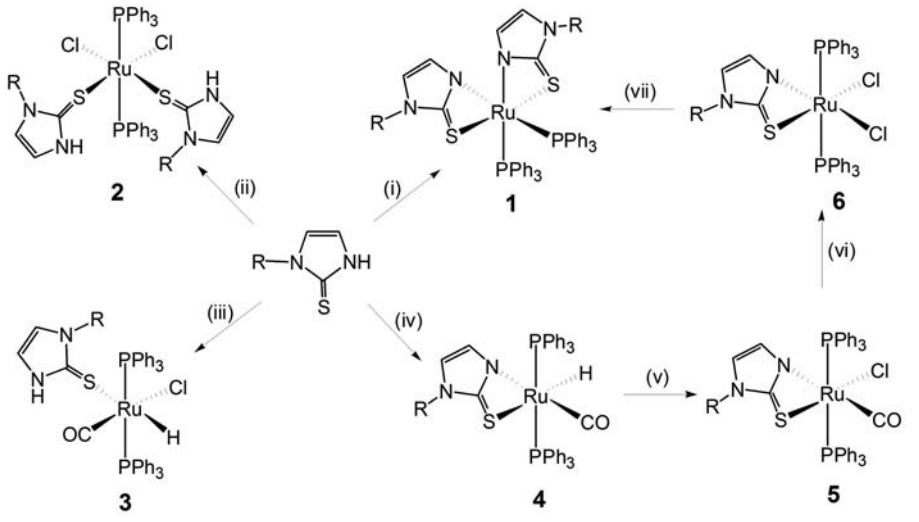

Scheme 1. Reactions between the $Himt^{MPh}$ or $Himt^{NPh}$ and the starting ruthenium compounds, and the reactivity of the ruthenium hydride and carbonyl complexes. Reagents and conditions: (a) $[Ru(PPh_3)_3Cl_2]$/NaOMe, THF, room temperature (r.t.); (b) $[Ru(PPh_3)_3Cl_2]$, THF, r.t.; (c) $[RuHCl(CO)(PPh_3)_3]$, THF, r.t.; (d) $[RuHCl(CO)(PPh_3)_3]$/NaOMe, THF, r.t.; (e) $CHCl_3$, reflux; (f) $CHCl_3$, *hr*, r.t.; (g) excess $Himt^{MPh}$/NaOMe, $CHCl_3$, reflux.

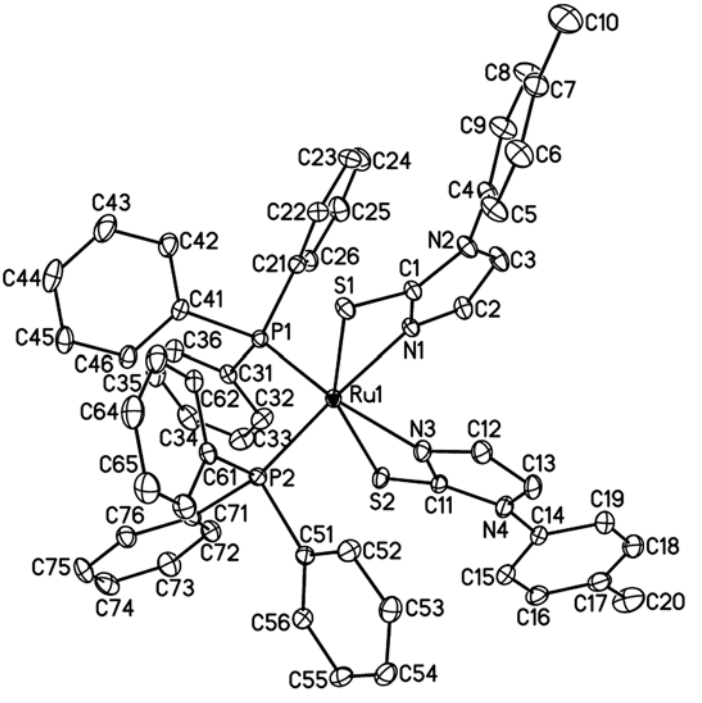

Figure 1. Molecular structure of *cis*-$[Ru(PPh_3)_2(\kappa^2\text{-}S,N\text{-}imt^{MPh})_2]$, **1**. Selected bond lengths (Å) and angles (°): Ru(1)–S(1) 2.486(3), Ru(1)–S(2) 2.473(3), Ru(1)–N(1) 2.133(4), Ru(1)–N(3) 2.164(4), Ru(1)–P(1) 2.305(3), Ru(1)–P(2) 2.308(3); N(1)–Ru(1)–N(3) 78.9(2), N(3)–Ru(1)–P(2) 92.3(1), N(1)–Ru(1)–P(1) 91.1(1), N(1)–Ru(1)–S(1) 68.0(1), N(3)–Ru(1)–S(1) 88.8(1), P(2)–Ru(1)–S(1) 101.9(1), P(1)–Ru(1)–S(1) 95.9(1), N(1)–Ru(1)–S(2) 91.5(1), N(3)–Ru(1)–S(2) 67.3(1), P(2)–Ru(1)–S(2) 94.5(1), P(1)–Ru(1)–S(2) 104.3(1), P(1)–Ru(1)–P(2) 99.0(1).

gave the ruthenium hydride complex [RuH(κ^2-*S*,*N*-imt)(CO)-(PPh_3)$_2$] (**4**). Similar [RuH(κ^2-*S*,*N*-tim^{Me})(CO)(PPh_3)$_2$)] (tim^{Me} = 1-methyl-2-mercaptoimidazole) was previously reported [13]. Complexes **4a** and **4b** easily converted to their corresponding ruthenium chloride complexes [RuCl(κ^2-*S*,*N*-imt^{MPh})(CO)(PPh_3)$_2$] (**5a**) and [RuCl(κ^2-*S*,*N*-imt^{NPh})(CO)(PPh_3)$_2$] (**5b**), respectively, in refluxing $CHCl_3$ by chloride substitution of RuH. Photolysis of **5a** in $CHCl_3$ at room temperature afforded a highly air-sensitive orange species which quickly turned green. An X-ray diffraction study revealed that the photo-substitution of [RuCl(κ^2-*S*,*N*-mim^{MPh})(CO)(PPh_3)$_2$] (**5a**) led to an oxidized product [$RuCl_2$(κ^2-*S*,*N*-imt^{MPh})(PPh_3)$_2$] (**6**) with chloride arising from $CHCl_3$. The mechanism for the formation of the ruthenium(III) complex is unclear but probably involves the ruthenium(II) oxidation during the photo-substitution. Interaction of **6** with 2 equiv. Na[imt^{MPh}] at reflux led to change from green to orange red, from which orange crystals formed, indentified as **1** by using unit cell measurement and elemental analyses. Obviously, the reaction involved reduction in ruthenium(III) to ruthenium(II) and substitution of chloride by [imt^{MPh}]$^-$, suggesting that [Ru(PPh_3)$_2$] in **5a** was reduced by the excess ligand and further resulted in formation of the thermodynamic **1**.

IR spectra of **2** and **3** clearly show weak bands at 3150 and 3137 cm^{-1}, respectively, attributed to ν(N–H). Similarly, ^{1}H NMR spectra of **2** and **3** showed proton resonances of NH as broad singlet at 11.64 and 12.68 ppm, respectively. The terminal carbonyl stretching vibrations were found at 19191940 cm^{-1} in IR spectra of **3–5**. One ^{31}P signal in ^{31}P NMR spectra of **2** (29.3 ppm), **3** (40.9 ppm), **4a** (39.3 ppm), **4b** (39.2 ppm), **5a** (38.4 ppm), and **5b** (38.2 ppm) is due to *trans* PPh_3; the ^{31}P NMR spectrum of **1** showed ^{31}P signals as

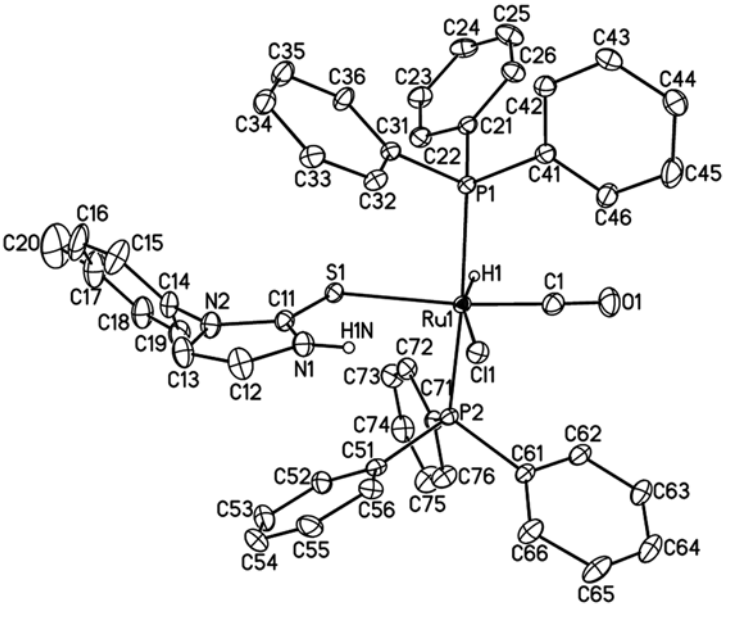

Figure 2. Molecular structure of [RuHCl(CO)(κ^1-*S*-$Himt^{MPh}$)(PPh_3)$_2$], **3**. Selected bond lengths (Å) and angles (deg): Ru(1)–H(1) 1.59(3), Ru(1)–C(1) 1.832(8), Ru(1)–S(1) 2.478(2), Ru(1)–P(1) 2.371(2), Ru(1)–P(2) 2.366(2), Ru(1)–Cl(1) 2.539(1); C(1)–Ru(1)–P(1) 92.9(2), C(1)–Ru(1)–P(2) 90.5(2), C(1)–Ru(1)–Cl(1) 99.1(2), P(1)–Ru(1)–Cl(1) 90.4(1), P(2)–Ru(1)–Cl(1) 91.6(1), P(1)–Ru(1)–S(1) 88.6(1), P(2)–Ru(1)–S(1) 87.4(1), Cl(1)–Ru(1)–S(1) 101.6(1), C(1)–Ru(1)–H(1) 66.3(11), P(1)–Ru(1)–H(1) 88.2(11), P(2)–Ru(1)–H(1) 90.8(11), S(1)–Ru(1)–H(1) 93.0 (11), P(1)–Ru(1)–P(2) 175.7(4), Ru(1)–C(1)–O(1) 175.5(6).

two singlets (29.2, 55.6 ppm) due to *cis* PPh_3. ^1H NMR spectra of **3** and **4** displayed characteristic hydride resonances at −14.0 ppm as a triplet with coupling constant J_{HP} about 22.5 Hz. Magnetic susceptibility measurements in the solid state showed that **6** is paramagnetic with one unpaired electron, consistent with the trivalent ruthenium (low-spin d^5, $S = {}^1/_2$). The positive ion FAB mass spectra of **1**–**6** display the expected peaks corresponding to the molecular ions [(M^+), (M^+ – Cl) or (M^+ – L) or (M^+ – CO), and (M^+ – PPh_3)] with the characteristic isotopic distribution patterns.

The structures of **1**·EtOH, **3**·C_6H_{14}, **4b**·0.25CH_3COCH_3, and **6**·2CH_2Cl_2 have been established by X-ray crystallography. As shown in figure 1, the central ruthenium in **1** is octahedral, containing two $[imt^{MPh}]^-$ with N–Ru–S bite angles (av. 67.7(1)°) and two mutually *cis* PPh_3 ligands with a P–Ru–P bond angle of 99.0(1)°. The average Ru–S and Ru–N bond lengths in **1** are 2.480(3) and 2.148(4) Å, respectively, which are comparable with those in [Ru(κ^2-*S*,*N*-tim^{Me})$_2$(PPh_3)$_2$] (av. Ru–S = 2.478(1) Å and av. Ru–N = 2.164(3) Å) [10]. The molecular structures of [RuHCl(κ^1-*S*-$Himt^{MPh}$)(CO)(PPh_3)$_2$] (**3**) and [RuH(κ^2-*S*,*N*-$Himt^{NPh}$)(CO)(PPh_3)$_2$] (**4b**) are displayed in figures 2 and 3, respectively. The geometry around ruthenium in both ruthenium hydride complexes is *pseudo*-octahedral with two *trans*-binding PPh_3 ligands with P–Ru–P angles of 175.7(2)° for **3** and 175.72(4)° for **4b**. The terminal Ru–S bond length of 2.478(2) Å in **3** is similar to that of 2.480(3) Å (av.) in **1**. The N–Ru–S bite angle of 65.3(1)° in **4b** with two *trans*-PPh_3 is slightly less than that of 67.7(1)° (av.) in **1** with two *cis*-PPh_3. The Ru–H bond lengths of 1.59(3) Å in **3** and 1.59(3) Å in **4b** are within the ranges reported for ruthenium hydride complexes [10, 33]. Ru–C bond lengths (1.832(8) Å in **3** and 1.832(2) Å in **4b**) and Ru–C–O bond angles

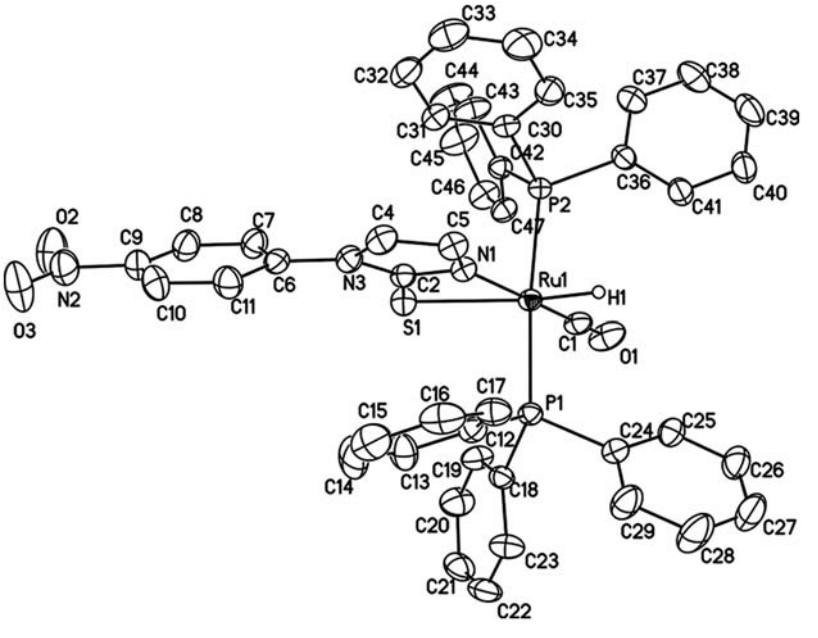

Figure 3. Molecular structure of [RuH(CO)(PPh_3)$_2$(κ^2-*S*,*N*-imt^{NPh})], **4b**. Selected bond lengths (Å) and angles (deg): Ru(1)–H(1) 1.59(3), Ru(1)–C(1) 1.832(3), Ru(1)–N(1) 2.138(2), Ru(1)–S(1) 2.619(1), Ru(1)–P(1) 2.359(1), Ru(1)–P(2) 2.346(1); C(1)–Ru(1)–N(1) 176.0(1), C(1)–Ru(1)–P(1) 92.2(1), C(1)–Ru(1)–P(2) 89.7(1), C(1)–Ru(1)–H(1) 90.5(1), P(1)–Ru(1)–H(1) 84.2(11), P(2)–Ru(1)–H(1) 88.8(11), C(1)–Ru(1)–S(1) 110.9(1), P(1)–Ru(1)–S(1) 93.8(2), P(2)–Ru(1)–S(1) 92.2(2), P(1)–Ru(1)–N(1) 89.6(1), P(2)–Ru(1)–N(1) 89.0(1), H(1)–Ru(1)–N(1) 93.3(10), S(1)–Ru(1)–N(1) 65.3(1), P(1)–Ru(1)–P(2) 172.7(2), Ru(1)–C(1)–O(1) 178.9(3).

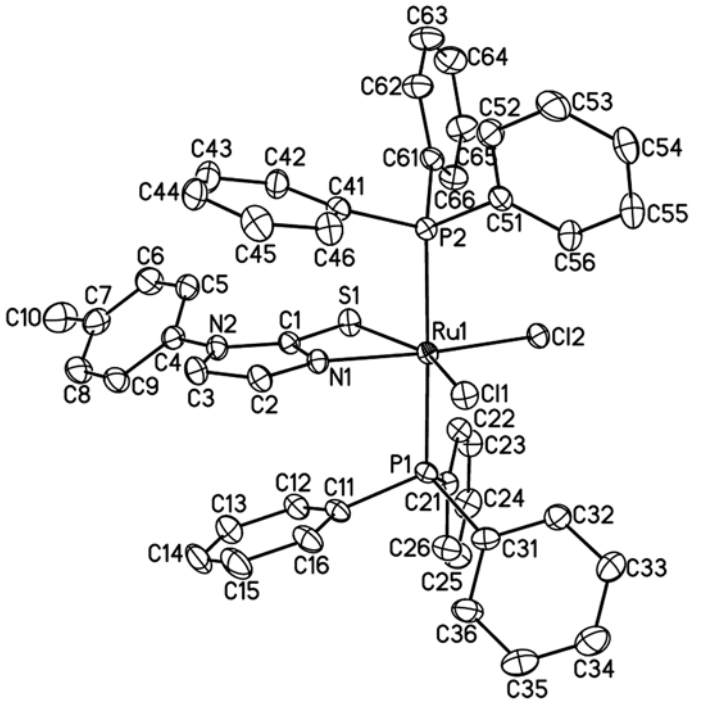

Figure 4. Molecular structure of $[RuCl_2(PPh_3)_2(\kappa^2\text{-}S,N\text{-}imt^{MPh})]$, **6**. Selected bond lengths (Å) and angles (deg): Ru(1)–S(1) 2.478(1), Ru(1)–N(1) 2.466(1), Ru(1)–Cl(1) 2.339(1), Ru(1)–Cl(2) 2.348(1), Ru(1)–P(1) 2.403(1), Ru(1)–P(2) 2.405(2); N(1)–Ru(1)–Cl(1) 90.6(1), Cl(1)–Ru(1)–Cl(2) 100.7(1), N(1)–Ru(1)–P(1) 90.6(1), Cl(1)–Ru(1)–P(1) 91.0(1), Cl(2)–Ru(1)–P(1) 89.5(1), N(1)–Ru(1)–P(2) 88.3(1), Cl(1)–Ru(1)–P(2) 89.0(1), Cl(2)–Ru(1)–P(2) 91.7(1), P(1)–Ru(1)–P(2) 178.8(1), N(1)–Ru(1)–S(1) 67.7(1), Cl(1)–Ru(1)–S(1) 158.2(1), Cl(2)–Ru(1)–S(1) 101.0(1), P(1)–Ru(1)–S(1) 87.7(1), P(2)–Ru(1)–S(1) 91.8(1).

(175.5(6)° in **3** and 178.9(3)° in **4b**) are normal for related ruthenium carbonyl complexes [34]. The molecular structure of $[RuCl_2(\kappa^2\text{-}S,N\text{-}imt^{MPh})(PPh_3)_2]$ (**6**) is illustrated in figure 4. The central ruthenium of **6** is octahedral, containing one chelating $[imt^{MPh}]^-$, two mutually *trans* PPh_3 and two mutually *cis* chlorides. The $[imt^{MPh}]^-$ binds to ruthenium in a *N*, *S*-bidentate mode with a N(1)–Ru(1)–S(1) bite angle of 67.7(1)°. The Ru–P bond length of 2.404(1) Å (av.) and the Ru–Cl bond length of 2.344(1) Å in **6** are slightly shorter than 2.406(1) Å and 2.376(1) Å, respectively, in $[RuCl_2(S_2CNMe_2)(PPh_3)_2]$ [23].

In summary, a series of ruthenium complexes with *N*-aryl-2-mercaptoimidazolyl ligands were synthesized and characterized. The ruthenium hydride carbonyl complexes converted to their corresponding ruthenium chloride complexes in refluxing chloroform. Photolysis of $[RuCl(\kappa^2\text{-}S,N\text{-}imt^{MPh})(CO)(PPh_3)_2]$ led to an oxidized ruthenium(III) complex $[Ru^{III}Cl_2(PPh_3)_2(\kappa^2\text{-}S,N\text{-}imt^{MPh})]$ which could be reduced to the ruthenium(II) complex *cis*-$[Ru(\kappa^2\text{-}S,N\text{-}imt^{MPh})_2(PPh_3)_2]$ in the presence of excess $[imt^{MPh}]^-$.

Supplementary material

Crystallographic data for **1**·EtOH, **3**·C_6H_{14}, **4b**·0.25CH_3COCH_3, and **6**·2CH_2Cl_2 have been deposited with the Cambridge Crystallographic Data Center as supplementary publication Nos. CCDC 813248–813252, respectively. Copies of the data can be obtained free of

charge on application to CCDC, 12 Union Road, Cambridge CB2 1EZ, UK [Fax: (+44) 1233-336-033; E-mail: deposit@ccdc.cam.ac.uk].

Acknowledgment

This project was supported by the Natural Science Foundation of China (Grant Nos. 20771003 and 21201003).

References

[1] M.C. Rodrigues-Arguells, M.B. Ferrari, G.G. Fava, G. Pelizzi, P. Tarasconi, R. Albertini, P.P. Dall'Aglio, P. Lunghi, S. Pinelli. *J. Inorg. Biochem.*, **58**, 157 (1995).
[2] E.S. Raper. *Coord. Chem. Rev.*, **153**, 199 (1996).
[3] S.B. Padhye, G.B. Kauffman. *Coord. Chem. Rev.*, **63**, 127 (1985).
[4] D.X. West, A.E. Liberta, S.B. Padhye, R.C. Chilate, P.B. Sonawane, A.S. Kumbhar, R.G. Yerande. *Coord. Chem. Rev.*, **123**, 49 (1993).
[5] D.X. West, S.B. Pahye, P.B. Sonawane. *Struct. Bonding (Berlin)*, **76**, 4 (1991).
[6] M.B. Ferrair, G.G. Fava, G. Tarsconi, R. Albertini, S. Pinelli, R. Starcich. *J. Inorg. Biochem.*, **53**, 13 (1994).
[7] A. Cingolani, E.F. Marchetti, C. Pettinari, B.W. Skelton, A.H. White. *Inorg. Chem.*, **41**, 1151 (2002).
[8] Y. Matsunaga, K. Fujisawa, N. Amir, Y. Miyashita, K.-I. Okamoto. *J. Coord. Chem.*, **58**, 1047 (2005).
[9] F. Isaia, M.C. Aragoni, A. Garau, V. Lippolis, A. Pintus. *Dalton Trans.*, **40**, 4505 (2011).
[10] R.D. Dewhurst, A.R. Hansen, A.F. Hill, M.K. Smith. *Organometallics*, **25**, 5843 (2006).
[11] M. Jimenez-Tenorio, M.C. Puerta, P. Valerga. *Organometallics*, **28**, 2787 (2009).
[12] J.G. Melnick, K. Yurkerwich, G. Parkin. *Inorg. Chem.*, **48**, 6763 (2009).
[13] J.D.E.T. Wilton-Ely, S.J. Honarkhah, M. Wang, D.A. Tocher, A.M.Z. Slawin. *Dalton Trans.*, 1930 (2005).
[14] F.A. Cotton, G. Wilkinson, *Advanced Inorganic Chemistry*, 5th Edn., p. 1097, John Wiley & Sons, New York (1988).
[15] H.W. Walker, R.G. Pearson, P.C. Ford. *J. Am. Chem. Soc.*, **105**, 1179 (1983).
[16] M.R. Torres, A. Vegas, A. Santos, J. Ros. *J. Organomet. Chem.*, **309**, 169 (1986).
[17] N. Mathew, B.R. Jagirdar, A. Ranganathan. *Inorg. Chem.*, **42**, 187 (2003).
[18] S.-I. Murahashi, H. Takaya, T. Naota. *Pure Appl. Chem.*, **74**, 19 (2002).
[19] S. Omura, T. Fukuyama, J. Horiguchi, Y. Murakami, I. Ryu. *J. Am. Chem. Soc.*, **130**, 14094 (2008).
[20] T. Kuwahara, T. Fukuyama, I. Ryu. *Org. Lett.*, **14**, 4703 (2012).
[21] S.-I. Murahashi, S. Sasao, E. Saito, T. Naota. *J. Org. Chem.*, **57**, 2521 (1992).
[22] X. Liu, Q.F. Zhang, W.H. Leung. *J. Coord. Chem.*, **58**, 1299 (2005).
[23] F.H. Wu, T. Duan, L. Lu, Q.F. Zhang, W.H. Leung. *J. Organomet. Chem.*, **694**, 3844 (2009).
[24] A.Q. Jia, Q. Ma, Q. Chen, H.T. Shi, W.H. Leung, Q.F. Zhang. *J. Organomet. Chem.*, **705**, 34 (2012).
[25] Q. Ma, A.Q. Jia, Q. Chen, H.T. Shi, W.H. Leung, Q.F. Zhang. *J. Organomet. Chem.*, **716**, 182 (2012).
[26] K. Matsuda, I. Yanagisawa, Y. Isomura. *Synth. Commun.*, **27**, 3565 (1997).
[27] T.A. Stephenson, G. Wilkinson. *J. Inorg. Nucl. Chem.*, **28**, 945 (1966).
[28] N. Ahmad, J.J. Levison, S.D. Robinson, M.F. Uttley, E.R. Wonchoba, G.W. Parshall. *Inorg. Synth.*, **15**, 45 (1974).
[29] *SMART and SAINT+ for Windows NT Version 6.02a.* Bruker Analytical X-ray Instruments Inc., Madison, Wisconsin, USA (1998).
[30] G.M. Sheldrick. *SADABS*, University of Göttingen, Germany (1996).
[31] G.M. Sheldrick. *SHELXTL Software Reference Manual. Version 5.1*, Bruker AXS Inc., Madison, Wisconsin (1997).
[32] G.M. Sheldrick. *Acta Crystallogr., Sect. A*, **64**, 112 (2008).
[33] M.S.-J. Foreman, A.F. Hill, G.R. Owen, A.J.P. White, D.J. Williams, G.R. Owen. *Organometallics*, **22**, 4446 (2003).
[34] P. Kumar, M. Yadav, A.K. Singh, D.S. Pandey. *J. Organomet. Chem.*, **695**, 994 (2010).